



LAWRENCE
LIVERMORE
NATIONAL
LABORATORY

Validation of a 3-D, Thermo-Mechanically Coupled Model for Multi-Pass Rolling in a Reversing Mill

M. Rhee, P. Wang, M. Li, R. Becker

June 14, 2004

The 8th International Conference on Numerical Methods in Industrial Forming Processes

The Ohio State University
Columbus, Ohio
June 13-17. 2004

This document was prepared as an account of work sponsored by an agency of the United States Government. Neither the United States Government nor the University of California nor any of their employees, makes any warranty, express or implied, or assumes any legal liability or responsibility for the accuracy, completeness, or usefulness of any information, apparatus, product, or process disclosed, or represents that its use would not infringe privately owned rights. Reference herein to any specific commercial product, process, or service by trade name, trademark, manufacturer, or otherwise, does not necessarily constitute or imply its endorsement, recommendation, or favoring by the United States Government or the University of California. The views and opinions of authors expressed herein do not necessarily state or reflect those of the United States Government or the University of California, and shall not be used for advertising or product endorsement purposes.

Validation of a 3-D, Thermo-Mechanically Coupled Model for Multi-Pass Rolling in a Reversing Mill

Moono Rhee*, Paul Wang**, Ming Li** and Richard Becker*

* *Lawrence Livermore National Laboratory, Livermore, CA, 94550*

** *Alcoa Technical Center, Alcoa Center, PA, 15069*

Abstract. A three dimensional numerical model simulating multi-pass, hot rolling on a reversing mill has been developed to analyze deformation patterns and shape changes of a rolled ingot. Validation simulations through 15 passes with an 86% reduction have been performed using the thermo-mechanically coupled model to track the evolution of the deformed ingot geometry. The heat transfer coefficient for thermal conduction between the rolls and slab has been estimated in accordance with experimental data, and heat transfer to the air and coolant outside of the roll bite is included. A hyperbolic sine model using the Zener-Hollomon parameter is used to capture the temperature and strain rate dependence of the aluminum alloy. A Coulomb friction model with a flow strength dependent maximum limit on the interfacial shear stress was employed between the rolls and ingot. Results of validation simulations and comparisons with experiments focusing on the ingot shape evolution are discussed.

INTRODUCTION

Due to the severe reduction and heat transfer during hot rolling, understanding the thermo-mechanical history of the material is essential for production of the final slab material with desired thickness and properties. Modeling of the multi-pass hot rolling process requires knowledge of several technical aspects: constitutive models for the material, thermal properties, thermal boundary conditions, interface heat conduction and interface friction. Because the large deformation and stress and temperature gradients encountered in the slab can lead to failure, fracture models are also necessary. These individual topics have been studied by many researchers, and there is ample literature on these subjects [1-3].

However, due to heavy computer power required for the lengthy simulations, numerical studies integrating these models are limited and usually reduced to two-dimensional or steady state simulations. Although analyses based on 2D models and steady state models are satisfactory for many problems, the 3D and transient nature of the problems encountered in rolling processes such as slab bulge behavior [4], center and surface inhomogeneous appearance would require 3D transient models.

With the advent of ever-increasing computer power and larger memory, large-scale rolling process models which require significant computational resources can be tractable using moderately sized

parallel computer systems [2]. In this paper, a three-dimensional finite element model utilizing staggered thermo-mechanical coupling is used to simulate a hot rolling process through a reversing mill. The work focuses on validation of the slab shape evolution for a complete pass schedule (13 passes) by comparing with experimental results. The goals of this work are to be able to predict temperature, strain rate, and damage evolution within the work-piece as it evolves through the multi-pass rolling, and to determine the effect of the initial slab shape and rolling pass schedule on fracture and internal product integrity. This is a step toward using the full 3D capability for process optimization.

EXPERIMENTAL

Tension tests conducted at high temperatures are used to determine the constitutive response and the strain to fracture for three different Al-Mg 5xxx alloys at various temperatures and strain rates. Tensile specimens were fabricated from rolled slabs along the through-thickness direction. The orientation is such that strength and ductility in the thickness direction are measured. The dimensions of the cylindrical tensile specimens are 0.572 cm diameter and 3.1 cm gauge length. A thermocouple is inserted in the end of the tensile specimen, and is used to control the temperature prior to the test. The apparatus used for the tensile tests is represented schematically in Figure 1. It is composed of two frames which slide relative to each other when

loaded by a compressive ram. The specimen threaded to each frame is subject to a tensile force.

The samples were deformed in tension under uniaxial stress at isothermal and constant true strain rate conditions using a servo-hydraulic controlled tester. Control of true strain rate is based on real time calculation of ram velocity proportional to the current gauge length. Assuming the tensile stretch is uniform throughout the gauge length, the logarithmic tensile strain is calculated with respect to the change of gauge length on a real time basis. Readers should refer to the work of Wang et al. [5] for more details on experimental procedures and results for fractography and microstructural characteristics.

FIGURE 1. Schematic of the tensile apparatus for elevated temperature testing.

CONSTITUTIVE RELATIONS

The strain rate and temperature effects on the flow stress are important for elevated-temperature deformation processing. The flow stress ($\bar{\sigma}$) and internal state variables evolution rates (S^r) are schematically represented as

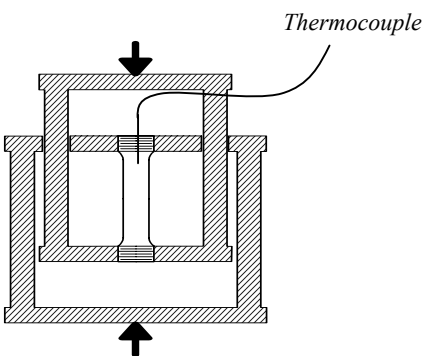
$$\bar{\sigma} = g(\dot{\varepsilon}, T, S^r, C^r) \quad (1)$$

$$\dot{S}^r = hr(\dot{\varepsilon}, T, S^r, C^r), \quad (2)$$

which depend on process variables such as strain rate ($\dot{\varepsilon}$) and temperature (T), the internal state variables (S^r), and the composition (C^r). At high temperatures and constant composition, the saturated stress $\bar{\sigma}^*$ as a function of temperature and strain rate is sufficient to describe the behavior of the Al-Mg alloys.

$$\bar{\sigma}^* = \frac{1}{\alpha} \sinh^{-1} \left[\left(\frac{Z}{A} \right)^{1/n} \right], \quad (3)$$

where



$$Z = \dot{\varepsilon} \exp\left(\frac{Q}{RT}\right). \quad (4)$$

Z is the temperature compensated strain rate (Zener-Hollomon parameter), Q the activation energy, R the gas constant and T the absolute temperature. The experimentally determined constants for 5xxx alloy used in the simulations are:

$$\begin{aligned} \alpha &= 0.04002 \text{ (MPa}^{-1}\text{)} \\ A &= \exp(20.43) \text{ (sec}^{-1}\text{)} \\ n &= 2.320 \\ Q &= 251000 \text{ (J/mole)} \end{aligned}$$

The flow stress decreases with increasing temperature and increases with increasing strain rates.

Fracture model

In bulk forming (e.g., rolling, extrusion, forging), material failure is generally complex and three-dimensional in nature. It depends on local stress states, strain rate, temperature, and microstructure features. Vujovic et al. [6] developed a fracture criterion based on the concept of forming limit curves. Alexandrov et al. [7,8] compared the criterion to experimental results of various die upsetting cases and found that the criterion incorporating a stress triaxiality factor was in good agreement with ductile fracture of steel at room temperature.

Experimental observation and data from tensile test results of Al-Mg alloys have provided the information needed to develop fracture criteria. The fracture behavior of Al-Mg alloys at elevated temperature could have at least two fracture modes – transgranular ductile fracture and hot shortness, a grain boundary failure mode. Fracture strain can be correlated with the temperature compensated strain rate, $\ln(Z)$, and hot ductility may shift from a ductile fracture mode to the hot shortness mode according to the strain rate and temperature. With increasing temperature in the hot shortness mode ductility drops rapidly.

Thus, the concept of developing multiple-mode fracture criterion has emerged from the data mentioned above, as illustrated in Figure 2. The schematic shows that the strain to fracture is bounded on one side by the temperature compensated strain rate, $\ln(Z)$, as the limit curve for the ductile fracture mode, while three little caps branching from the limit curve represent the other fracture response – the hot shortness mode, dictated by strain rate ($\dot{\varepsilon}$). This

schematic essentially represents a fracture limit diagram, similar to Vujovic et al. [6], but with the additions of $\ln(Z)$ and strain rate to capture the multiple fracture modes observed in Al-Mg alloys. Figure 2 only represents a fracture limit diagram under a constant stress triaxiality for uniaxial tensile response. A third axis could be added to the diagram to represent the stress triaxiality factor. This would require experimental data from torsion and compression tests.

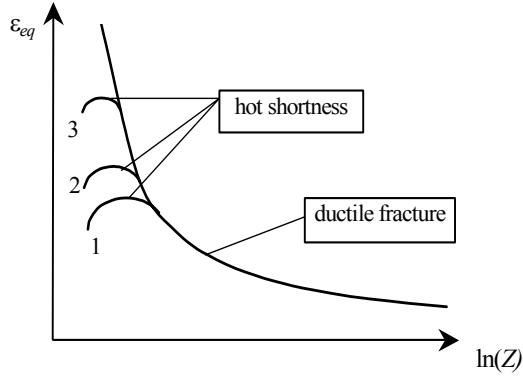


FIGURE 2. Schematic fracture criteria for Al-Mg alloys, at constant stress triaxiality showing the regimes of ductile fracture and hot shortness modes ($\dot{\epsilon}_1 > \dot{\epsilon}_2 > \dot{\epsilon}_3$).

According to the schematic shown in Figure 2, a ductility based fracture criterion, φ_f^i , as a function of stress triaxiality, strain rate, temperature, internal state variables, and composition is used for elevated temperature process modeling.

$$\varphi_f^i = f^i(\beta, \dot{\epsilon}, T, S^r, C^r) \quad (5)$$

where i represents the mode of fracture (ductile or hot shortness). β is the stress triaxiality factor defined by $\beta = \sigma_k / \bar{\sigma}$ where σ_k is the hydrostatic stress component. φ_f^i is the effective strain at fracture. It can be determined from simple deformation experiments such as tension, torsion and compression tests.

A path dependent effective strain quantity can be defined as:

$$\varepsilon_{eq} = \int_0^t \dot{\varepsilon}_{eq} dt \quad (6)$$

where $\dot{\varepsilon}_{eq} = \sqrt{(2/3)\dot{\varepsilon}_{ij}\dot{\varepsilon}_{ij}}$, $\dot{\varepsilon}_{ij}$ are the strain rate components, and t is the time. We also introduce a path dependent average value of β by:

$$\bar{\beta} = \varepsilon_{eq}^{-1} \int_0^t \beta \dot{\varepsilon}_{eq} dt \quad (7)$$

In the case of simple tests (uniaxial compression, uniaxial tension and pure torsion), the values of β and $\bar{\beta}$ coincide and are determined as -1, 1 and 0, respectively. Assuming S^r and C^r are constant, the multiple-mode fracture criterion of Al-Mg alloy is proposed as follows:

$$\varphi_f = A \begin{cases} f^D(\bar{\beta}, \ln Z), & \ln Z \geq \ln Z^{(0)} \\ f^S(\bar{\beta}, \ln Z, \dot{\varepsilon}_{eq}), & \ln Z^{(c)} \leq \ln Z \leq \ln Z^{(0)} \end{cases} \quad (8)$$

where $A = 2/(1 + \bar{\beta})$ and

$$\begin{aligned} f^D &= c_0 + c_1 \ln Z + c_2 \ln^2 Z + c_3 \ln^3 Z \\ f^S &= \varepsilon_0 (\ln Z - \ln Z^{(c)}) (\ln Z - \ln Z^{(x)}) \end{aligned} \quad (9)$$

with $c_0 = -3.614$, $c_1 = 0.586$, $c_2 = -0.0233$ and $c_3 = 2.87 \times 10^{-4}$ and ε_0 , $\ln Z^{(c)}$, and $\ln Z^{(x)}$ are constants and given in a tabular form in [5].

Friction Model

The most commonly used friction model at contact interface regions is the Amontons-Coulomb friction law $\tau_f = \mu p$, where the constant of proportionality μ is the coefficient of friction [8] and p is the interface pressure. Another expression that is widely accepted for use in the metal forming industry is given by $\tau_f = m \tau_y$, where m is the friction factor and τ_y is the yield stress of the work-piece in shear. The friction model in our study is a combination of the two based on the Coulomb-type friction with a flow stress dependent maximum limit on the interfacial shear stress. It is given as:

$$\tau_f = \begin{cases} \mu p & \text{if } p < \frac{m}{\mu} \tau_y(\dot{\varepsilon}, T) \\ m \tau_y(\dot{\varepsilon}, T) & \text{if } p > \frac{m}{\mu} \tau_y(\dot{\varepsilon}, T) \end{cases} \quad (10)$$

Although more complex models may be necessary when conditions such as geometry and roll speed become sensitive to lubrication conditions, it is generally assumed that the value of friction factor or friction coefficient is independent of geometric constraints. Other models used in forming processes

include modified versions of the Coulomb type friction model by using more complex functions of the roll pressure for the friction stress (see, for example, [10,11]). In our simulations, the values of μ and m are 0.4 and 0.8, respectively.

Heat Transfer Coefficient

The heat transfer coefficient between the roll and the slab can largely depend on specific rolling conditions such as roll speed and geometry, reduction, contact time and material [3]. Thermal boundary conditions used in the simulation include conductance at contact region and convection to the air and coolant as schematically shown in Figure 3. The interface heat transfer coefficient used in the simulations is estimated in accordance with experimental data using a laboratory mill. The specific heat, thermal conductivity and density of the 5xxx aluminum alloy were based on experimental data.

The thermal conductivity of the slab is expressed as a function of temperature in a power law form fitted from the experimental data. A textbook value $h \sim 10 \text{ W}/(\text{m}^2 \cdot ^\circ\text{K})$ is assumed for the convection coefficient to air. Thermal diffusion occurs continuously. An iterative trial-and-error method is employed to estimate the heat transfer coefficient (h) for the reversing mill experiments. The value we found for h is $150 \text{ W}/(\text{m}^2 \cdot ^\circ\text{K})$.

NUMERICAL CALCULATIONS

The finite element program used for the simulations is ALE3D [12]. This is an arbitrary Eulerian and Lagrangian multi-physics program that can perform simulations for visco-plastic deformation combined with chemistry and heat transfer models. It is designed for efficient use on massively parallel computer platforms.

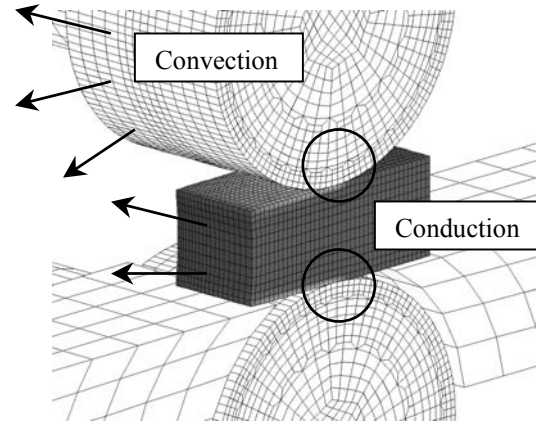


FIGURE 3. Thermal boundary conditions: conduction at the contact region, convection and diffusion.

The initial geometry for the laboratory scale reversing mill simulations consists of top and bottom steel rolls, the run-out table and a 5xxx aluminum alloy slab as shown in Figure 4. The diameters of the top and bottom rolls are 0.5923 m and 0.5893 m . The dimensions of the slab are 0.1778 m in thickness, 0.4318 m in length and 0.3556 m in width. The initial temperature of the slab immediately emerging from furnace is 998 K and the rolls are initially 300 K . To account for deformation and heat transfer, a staggered thermo-mechanically coupled strategy is employed. The time integration scheme adopted for the mechanical calculation is explicit with mass scaling, while that for the heat transfer calculation is implicit. The computational cost per time step for the implicit thermal calculation is higher than for the explicit mechanical calculations. Since larger time steps can be employed when solving the heat transfer equation, the thermal part of the simulation is solved once for every 10-20 explicit calculations in order to improve computational efficiency.

At the end of each pass, the direction of the slab is reversed, and the rolls repositioned for further reduction, in accordance with the pass schedule. Continuous cooling occurs by convective heat transfer while the rolls are adjusted. The temperature of the slab decreases due to convection to air and thermal conduction from the slab to the cold rolls during the pass. At intervals of 4 passes in the experiment, the slab was reheated in a furnace to maintain a suitable deformation temperature. The reheating is captured in the model by setting the slab surface temperature to a desired level and allowing enough time for a uniform temperature to be reached throughout the slab. The roll temperature is reset to ambient temperature. Since it is not known how far

the coolant flows onto the slab, the net cooling effect is approximated. The deformation heating is found to be approximately a 5 to 10 degrees Celsius increase per pass.

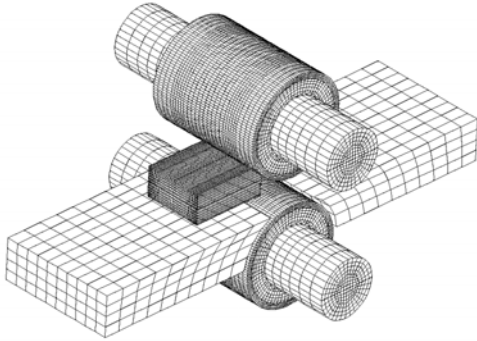


FIGURE 4. Initial Rolling geometry.

Remeshing

One important aspect observed during the simulation is that the quality of the mesh degraded by the 7th pass and it rapidly became worse. A more accurate representation of the deformed slab is necessary to prevent misleading simulation results, particularly for the last few passes when element aspect ratios become excessive. A remeshing technique has been used to create a new mesh matching the deformed geometry, and a remapping utility [12] is employed to transfer the stress, state variables and temperature from the deformed configuration to the new mesh.

Shape Comparison

In order to validate the integrity of the models employed, the shape change evolution of the slab is compared with experimental results. Qualitative comparison of the sectional views of the leading edge at the center plane along the length of the slab at the end of the 8th pass for both experiment and simulation is given in Figure 5a). From Figure 5a), it can be seen that the curvature at the slab mouth at the centerline is slightly higher than the experimental result. This may reflect mesh resolution issues where the gradient at the midplane is not properly resolved. Simulation results of the slab side profiles at various

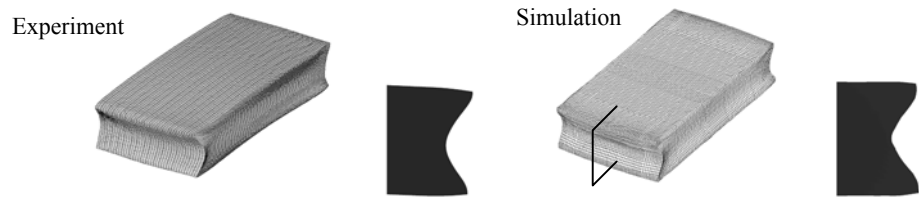
positions along the slab are given in Figure 5b). These show good agreement with the experimental results.

Results of ingot shape evolution for a 13 pass rolling simulation are given in Figure 6. In this model, it was observed that the rollover of the slab is strongly dependent on friction. Thus, using the simple Coulomb friction law with a maximum limit dependence on flow strength may not be sufficient. More studies on friction laws may be necessary for more accurate prediction. Another important feature that one should not neglect is the mesh dependence of the result. More frequent remeshing may be necessary to be able to capture the deformation behavior more accurately.

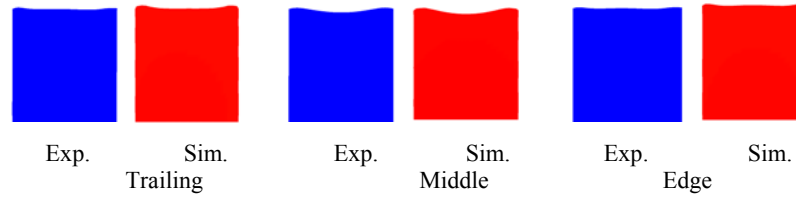
CONCLUSION

A multi-pass hot reversing mill process has been simulated, focusing on validation of the model by comparing slab shape evolution. Deformation history and temperature are the major factors that affect the final product integrity and shape in the rolling process. These are heavily influenced by interfacial friction and heat transfer during rolling. Mesh size can also play an important role in the simulated deformation of the slab. Another important issue that one cannot neglect in rolling processes is fracture behavior. Deformation process paths can be limited by damage and material failure.

The rollover of a slab edge during rolling is a three-dimensional process which requires moderately long computer simulations. Although the current model can predict the rollover within reasonable accuracy, more simulations are necessary to obtain optimum parameter values that would yield a quantitative prediction. Simulation results indicate that key parameters controlling the slab shape during or after deformation are mesh size and friction at the contact interface as well as thermal properties and damage. Parametric studies on these issues are currently underway and will be reported in a forthcoming paper.



a) Sectional views of the leading edge at the center plane along the length of the slab



b) Side profile comparison

FIGURE 5. Shape geometry at the end of 8th pass for experiment and simulation: a) Sectional view comparison of the leading edge at the centerline of the slab, and b) side profile comparison at trailing, middle and edge plane.

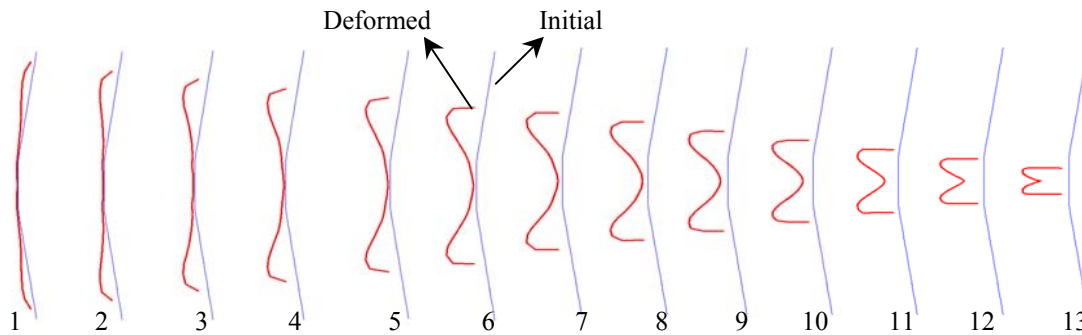


FIGURE 6. Simulation result of slab side profile evolution up to 13th pass.

ACKNOWLEDGMENT

This work was performed under the auspices of the U.S. Department of Energy by the University of California, Lawrence Livermore National Laboratory under Contract No. W-7405-Eng-48 and Alcoa corporate and plant research programs.

REFERENCES

1. Serajzadeh, S, Karimi Taheri, A. and Mucciardi, F., Modeling Simul. Mater. Sci. Eng., **10**, 185-203 (2002).
2. Duan, X. and Sheppard, T., Modeling Simul. Mater. Sci. Eng., **10**, 363-380 (2002).
3. Tseng, A.A., Numerical Heat Transfer, Part A, **35**, 115-133 (1999).
4. Lee, Y.S. and Dawson, P.R., *Int. J. Numer. Methods Eng*, **30**, 1403-1413 (1990).
5. Wang, P., Roadman, R.E., Jin, Z. and Alexandrov, S., Hot Deformation of Aluminum Alloy III, 483-497, 2003 TMS Annual Meeting Proceedings.
6. Vujovic, V. and Shabaik, A.H., *Trans. ASME J. Engn Mater. Struct.*, 1986, 108, 245-249.
7. Alexandrov, S., Chikanova, N. and Vilotic, D., In *Proc. 3rd Int. Conf. on Materials Processing Defects "Advanced Methods in Materials Processing Defects"* (Eds M. Predeleanu and P. Gilormini), Elsevier, Amsterdam, 1997, p. 247-256.
8. Vilotic, D., Chikanova, N. and Alexandrov, S., *J. of Strain Analysis*, **34**, 17-22 (1999).
9. Keife, H. and Sjogren, C., *Wear*, **179**, 137-142 (1994).
10. Wanheim, T., Bay, N., and Petersen, A. S., *Wear*, **28**, 251-258 (1974).
11. Keife, H. and Sjogren, C., *Wear*, **179**, 137-142 (1994).
12. ALE3D, Lawrence Livermore National Laboratory, (2003).